Preprint published in ***Magnetic Resonance in Medicine*** 64:9-14 (2010).

The original publication is available at
http://www3.interscience.wiley.com/journal/10005196/home
via the following DOI: http://dx.doi.org/10.1002/mrm.22480

Diffusion Imaging in Humans at 7T using Readout-Segmented EPI and GRAPPA

Robin M. Heidemann[1]*, David A. Porter[2], Alfred Anwander[1], Thorsten Feiweier[2], Keith Heberlein[2], Thomas R. Knösche[1], Robert Turner[1]

[1]Max Planck Institute for Human Cognitive and Brain Sciences, Leipzig, Germany

[2]Siemens Healthcare Sector, Erlangen, Germany

***Corresponding Author:**

Robin M. Heidemann Ph.D.
Max Planck Institute for Human Cognitive and Brain Sciences,
Department of Neurophysics,
Stephanstr. 1a,
04103Leipzig, Germany
Tel: +49 341 9940 2429
http://www.cbs.mpg.de/~heidemann

*Preprint submitted to **Magnetic Resonance in Medicine** as a communication.*

Final draft: February 2010

Key words:

readout-segmented EPI, parallel imaging, 2D navigator, multi-shot diffusion, DTI

Abstract

The Anatomical magnetic resonance imaging studies at 7T have demonstrated the ability to provide high quality images of human tissue in vivo. However, diffusion-weighted imaging at 7T is limited by the increased level of artifact associated with standard, single-shot, echo-planar imaging (EPI), even when parallel imaging techniques such as GRAPPA are used to reduce the effective echo spacing. Readout-segmented EPI in conjunction with parallel imaging has the potential to reduce these artifacts by allowing a further reduction in effective echo spacing during the EPI readout. This study demonstrates that this approach does indeed provide a substantial improvement in image quality by reducing image blurring and susceptibility-based distortions, as well as by allowing the acquisition of diffusion-weighted images with a high spatial resolution. A preliminary application of the technique to high resolution diffusion tensor imaging (DTI) provided a high level of neuroanatomical detail, which should prove valuable in a wide range of applications.

Introduction

MRI of humans at 7T can provide highly detailed anatomical brain images and perform localized fMRI with very high spatial resolution. However, it remains a challenge to acquire good quality diffusion-weighted (DW) images at ultra-high field strengths. Single-shot EPI (ss-EPI) is well established as the method of choice for diffusion-weighted imaging (DWI) and therefore for diffusion tensor imaging (DTI). This is due to its low sensitivity to the motion-induced phase errors that occur during diffusion sensitization of the MR signal. However, ss-EPI is prone to artifacts related to susceptibility changes at tissue interfaces and has a limited spatial resolution due to T2* relaxation. Parallel imaging can be used to improve the image quality of ss-EPI acquisitions [1], but there are still significant limitations, particularly at higher field strength. Susceptibility effects and T_2* blurring increase with field strength and therefore parallel imaging techniques with high acceleration factors (greater than four) are necessary to address these problems for high resolution DWI and DTI [2]. The shorter T_2 of brain tissue at 7T presents further difficulties by limiting the acquisition of data at long echo times. At lower field strengths, improved image quality has been demonstrated in several studies using a variety of multi-shot DW sequences, which correct for the shot-to-shot, spatially-varying phase errors caused by cardiac pulsation during diffusion preparation [3-6]. An additional technique that can be used with non-linear phase correction is readout-segmented EPI (rs-EPI). Following an initial description by Robson et al. [7], the method was further developed in subsequent work to include 2D navigator correction, parallel imaging and navigator-based reacquisition [8]. This study and related work [9] has demonstrated that this approach can produce high resolution diffusion-weighted images with a robust correction for motion-induced phase errors.

In the current study, this approach is applied to the acquisition of DW images at 7T. The technique is attractive at this field strength due to the small number of RF refocusing pulses, giving lower SAR and reduced sensitivity to B1 inhomogeneity compared to TSE-based sequences. Previous studies at lower field strengths have shown that rs-EPI with parallel imaging and a 2D navigator based reacquisition [8] substantially improves the image quality when compared to standard ss-EPI protocols with parallel imaging. The aim of this study was to investigate whether the same approach can be used to address the more severe level of artifact seen in diffusionweighted ss-EPI at 7T.

Methods

All experiments were performed on a 7T whole-body MR scanner (MAGNETOM 7T, Siemens Healthcare Sector, Erlangen, Germany) using a 24-element phased array head coil (Nova Medical, Wilmington, MA, USA). Scans were performed on two healthy volunteers and informed consent was obtained before each study. Multi-shot DW images were acquired using the rs-EPI sequence in conjunction with 2D navigator correction and parallel imaging [8]. The sequence also used a data reacquisition scheme that was based on an idea originally proposed by Nguyen et al. [10] in the context of 1D navigators. In the current study, the 2D navigator data in k-space were used during the measurement to control the reacquisition of readout segments with phase errors at high spatial frequency, which cannot be removed by the standard 2D navigator phase correction. This procedure, which is described in detail elsewhere [8], uses the distribution width of the navigator k-space data to identify acquisitions with high spatial frequency phase errors and then automatically reacquires these data. These high spatial frequency phase components correspond to shifts in the k-space data, whereby data can be shifted beyond the limits of the current readout segment. In this case, it is not possible to recover these missing data by applying a 2D phase-correction with the navigator. As demonstrated in previous studies [8], if these corrupt data are not discarded they can cause localized artifacts in the final image. Images were reconstructed on the scanner using standard hardware and a dedicated image reconstruction program. For all acquisitions, fat suppression was applied using the method proposed by Ivanov et al. [11], in which slice excitation bandwidths are manipulated to provide a spatial mismatch between excitation and refocusing pulses for the chemically shifted fat resonances. This was achieved by using an excitation RF pulse duration of 2.8 ms and refocusing RF pulse duration of 10.2 ms. The increased duration of the refocusing pulse had the additional advantage of reducing SAR, albeit with a small increase in echo time of about 5 ms. All GRAPPA reconstructions were performed with a 2D convolution kernel [12] with three source points along the readout direction and two source points along the phase encoding direction.

A direct comparison between rs-EPI and single-shot EPI (ss-EPI) was performed by acquiring trace-weighted images with both methods using the same nominal spatial resolution. In each case, one image was acquired with b = 0 and three images with a b-value of 1000 s/mm^2. The three diffusion-weighted images were acquired with mutually orthogonal diffusion gradient directions. Trace-weighted images were then generated by taking the geometric mean of these three images. The following parameters were used for both sequences: matrix 192x192, FOV 220 mm, slice thickness 3 mm, 21 slices, GRAPPA acceleration factor 3. The rs-EPI protocol used a TR of 2810 ms, a TE of 64 ms, 9 readout segments (or shots) and 2 averages. Scan time (including reference scans and 14 reacquisition scans) was 4 min 10 s. The ss-EPI protocol used a TR of 2100 ms, a TE of 64 ms, 6 averages and a scan time of 59 s. In addition, a high resolution rs-EPI sequence was used with a matrix of 314x314, an FOV of 220 mm, slice thickness 3 mm, TR 3000 ms, TE 70 ms, 15 readout segments and 3 averages. Scan time (including reference scans and 36 reacquisition scans) was 10 min 57 s.

The prototype sequence and image reconstruction program used in this study placed some limitations on the range of parameters that could be used for DTI acquisitions, so protocols were chosen to allow a preliminary evaluation of the technique with fewer slices and thicker slices than would be used in a standard DTI protocol. A high resolution rs-EPI sequence was used with two different imaging protocols, A and (B): matrix = 220x220 (230x230), FOV = 220 (230) mm, slice thickness = 3.0 (3.5) mm, 3 (9) slices, GRAPPA acceleration factor 3, TR = 1000 (1800) ms, TE = 70 (75) ms, 9 readout segments and 3 (2) averages. Diffusion weighting was performed along 12 (20) directions with a b-value of 1000 s/mm^2. Scan time (including all reference scans and reacquisition scans) was 7 min 3 s (13 min 40 s) min.

Results

Fig. 1 directly compares trace-weighted images at b = 1000 s/mm^2 obtained using ss-EPI and rs-EPI, each accelerated by a factor of three; an identical GRAPPA reconstruction procedure was used in each case, but for the rs-EPI sequence the GRAPPA auto-calibration signals (ACS) were acquired using a fully sampled version of the central readout segment (acquired in a single shot) and for the ss-EPI sequence the ACS were acquired using a 3-shot, interleaved EPI acquisition. Even with an acceleration of three, the ss-EPI acquisition at 7T suffers from significant image blurring. In addition, there are signal voids in the anterior region of the brain stem, close to the midline. The same slice acquired with rs-EPI (shown on the right side of Fig. 1) shows substantially less signal loss and reduced blurring with a higher level of anatomical detail, despite having the same nominal spatial resolution. As shown in Fig. 2, increasing the number of readout segments from 9 to 15 made it possible to acquire detailed, high resolution, trace-weighted images with an in-plane resolution of 0.7 mm.

Two slices from a single average of a DTI acquisition using protocol A are shown in Fig. 3 and the results of the corresponding DTI analysis of the 12 direction data-set are shown in Fig. 4. A color-coded fractional anisotropy (FA) map with overlaid vector-orientation (left side of Fig. 4) shows the radial anisotropy in several cortical regions. The corresponding anatomical image is shown on the right side of Fig. 4. Enlarged sections show the right precentral gyrus and the central sulcus. The gray-white matter interface in the precentral gyrus is outlined to emphasize the radial nature of the anisotropy in the cortex. Another DTI example acquired with protocol B with 20 diffusion-weighting directions is given in Fig. 5. Two groups of voxels with distinct diffusion orientations can be identified in the anterior limb of the internal capsule. The main bundle is oriented along the inferior-superior direction (blue) crossed by several bands of voxels with medio-lateral diffusion orientation (red). The structure crossing the main bundle corresponds to the striatal cell bridges between the caudate nucleus and the putamen.

Discussion

Single-shot EPI at ultra-high field strength suffers from geometric distortions and image blurring, even when parallel imaging is used to shorten the EPI readout train, as clearly seen on the left side of Fig. 1. The acceleration factor of three is insufficient to address these problems. Severe distortions are prominent, not only in the frontal lobe close to the paranasal sinuses, but also close to the brain stem. Image blurring prevents the red nuclei in the ss-EPI acquisition from being seen clearly, whereas they are clearly depicted in the rs-EPI image on the right side of Fig. 1 (highlighted by an arrow on the right side of the image). A second arrow (on the left side of the rs-EPI image) highlights the anterior commissure, which can be identified connecting the two cerebral hemispheres across the midline. Due to signal voids, this structure cannot be seen in the ss-EPI image. This study has also shown that rs-EPI can be used to acquire high-resolution, diffusion-weighted images with a high level of anatomical detail, such as the depiction of the optic radiation in the images of Fig. 2.

The non-averaged base images from the DTI studies (Fig. 3) show a high level of anatomical detail, which is also evident in the derived fractional anisotropy maps of Fig. 4. In these FA maps it is possible to clearly identify the radial anisotropy in the cortex. Although this has been observed in previous studies, it is rarely observed in such a uniform manner across a large region of cortex. This is depicted in the color coded FA map with overlaid vector-orientations (left side of Fig. 4). The corresponding anatomy is in good alignment with the color coded FA map, as shown in the enlarged sections where the gray-white matter interface, determined from the structural scans, is outlined on both images. The second DTI example, acquired with protocol B using 20 diffusion-weighting directions, also shows detailed neuroanatomical structure, such as the two populations of voxels with distinct diffusion orientation in the anterior limb of the internal capsule.

All DWI studies were performed with a b-value of 1000 s/mm^2. Larger b-values could be used, but this would result in a longer echo-time, which is especially problematic at ultra-high field strength, due to the relatively low T_2 values, unless a higher diffusion gradient strength can be used to reduce the duration of the diffusion preparation. In this context, the rs-EPI sequence has the advantage over ss-EPI of a much shorter echo-spacing, which results in a corresponding reduction in TE when the same resolution and phase-encoding partial Fourier factors are used. The rs-EPI protocols used in this study used a full k-space acquisition, which for the comparison with ss-EPI resulted in the same TE as the ss-EPI protocol with a 6/8 partial Fourier factor. At higher spatial resolutions, there are further benefits to the rs-EPI sequence because the increased resolution in the readout direction can be achieved by increasing the number of shots without changing the echo-spacing. The duration of the EPI readout is therefore independent of the resolution in the readout direction and varies linearly with the resolution in the phase-encoding direction (according to the increased number of echoes in the echo-train). In contrast, with the ss-EPI sequence, a longer echo-spacing is required when the resolution in the readout direction is increased, so that the duration of the EPI readout and consequently the TE increase more rapidly with increasing spatial resolution.

The prototype sequence and image reconstruction program used in this preliminary study require further development to make it possible to acquire and process the large volumes of raw data that are generated by high-resolution, multi-shot DTI using a large number of receiver channels and diffusion directions. The current limitation is due to the specific implementation of the reacquisition algorithm, which makes it necessary to keep the whole raw data set in the computer memory during image reconstruction, so that severely corrupted data sets can be easily replaced with less corrupted reacquired data, which are measured at the end of the scan. For the MR scanner used in this study, this restricted the amount of raw data to about 4 GB. Clearly, this limitation could be addressed by adding additional memory to the image reconstruction computer. However, a more elegant strategy may be to adopt a ‘sliding-window’ approach, in which the reacquisition is performed at intervals during the scan, so that some images can be calculated before the end of the measurement and the corresponding raw data can be deleted. This approach would have the additional advantage of reducing the image calculation time at the end of the scan and would also reduce motion artifacts that might arise in long acquisitions due to the time interval between the original and the reacquired data sets. Once these developments have taken place, the rs-EPI method should allow detailed DWI studies to be extended to larger regions of the brain using high isotropic spatial resolution and a large number of diffusion directions. In conclusion, readout-segmented EPI with GRAPPA and a 2D navigator based reacquisition enables high quality DW images to be acquired at 7T, which are well suited to high resolution DTI applications. The resulting diffusion tensor data will permit the detailed study of neuroanatomy in future work.

Acknowledgment

We are grateful for the support and technical contributions of Dr Heiko Meyer and Stefan Huwer from Siemens Healthcare.

REFERENCES

1. Griswold MA, Jakob PM, Chen Q, Goldfarb J, Manning WJ, Edelman RR, Sodickson DK. Resolution enhancement in single-shot imaging using simultaneous acquisition of spatial harmonics (SMASH). Magn Reson Med. 1999;41:1236-1245.

2. Heidemann RM, Anwander A, Feiweier T, Fasano F, Pfeuffer J, Knösche TR, Turner R. High Resolution Diffusion-Weighted Imaging in Human at 7T. NeuroImage 2009;47,S1:S73.
3. Pipe JG, Farthing VG, Forbes KP. Multishot diffusion-weighted FSE using PROPELLER MRI. Magn Reson Med. 2002;47:42-52.
4. Miller KL, Pauly JP. Nonlinear phase correction for navigated diffusion imaging. Magn Reson Med. 2003;50:343-353.
5. Liu C, Bammer R, Kim D, Moseley ME. Self-navigated interleaved spiral (SNAILS): Application to high-resolution diffusion tensor imaging. Magn Reson Med. 2004;52:1388-1396.A
6. Atkinson D, Counsell S, Hajnal JV, Batchelor PG, Hill DL, Larkman DJ. Nonlinear phase correction of navigated multi-coil diffusion images. Magn Reson Med. 2006;56:1135-1139.
7. Robson MD, Anderson AW, Gore JC. Diffusion-weighted multiple-shot echo planar imaging of humans without navigation. Magn Reson Med. 1997;38:82-88.
8. Porter DA, Heidemann RM. High Resolution Diffusion-Weighted Imaging using Readout-Segmented Echo Planar Imaging, Parallel Imaging and a twodimensional Navigator-Based Reacquisition. Magn Reson Med. 2009;62:468-475.
9. Holdsworth SJ, Skare S, Rexford DN, Bammer R. Robust GRAPPA-Accelerated Diffusion-Weighted Readout-Segmented (RS)-EPI. Magn Reson Med. 2009;62:1629-1640.
10. Nguyen Q, Clemence M, Ordidge RJ. The use of intelligent re-acquisition to reduce scan time in MRI degraded by motion. In: Proceedings of the 6th Annual Meeting of ISMRM, Sydney, Australia, 1998. p 134.

11. Ivanov D, Schaefer A, Streicher M, Trampel R, and Turner R. Fat Suppression with Low SAR for SE EPI fMRI at 7T. In: Proceedings of the 17th Annual Meeting of ISMRM, Honolulu, USA, 2009. p. 1547.
12. Griswold MA. Advanced k-space techniques. In: Proceedings of the 2nd International Workshop on Parallel Imaging, Zuerich, Switzerland, 2004. p 16-18.

Figures

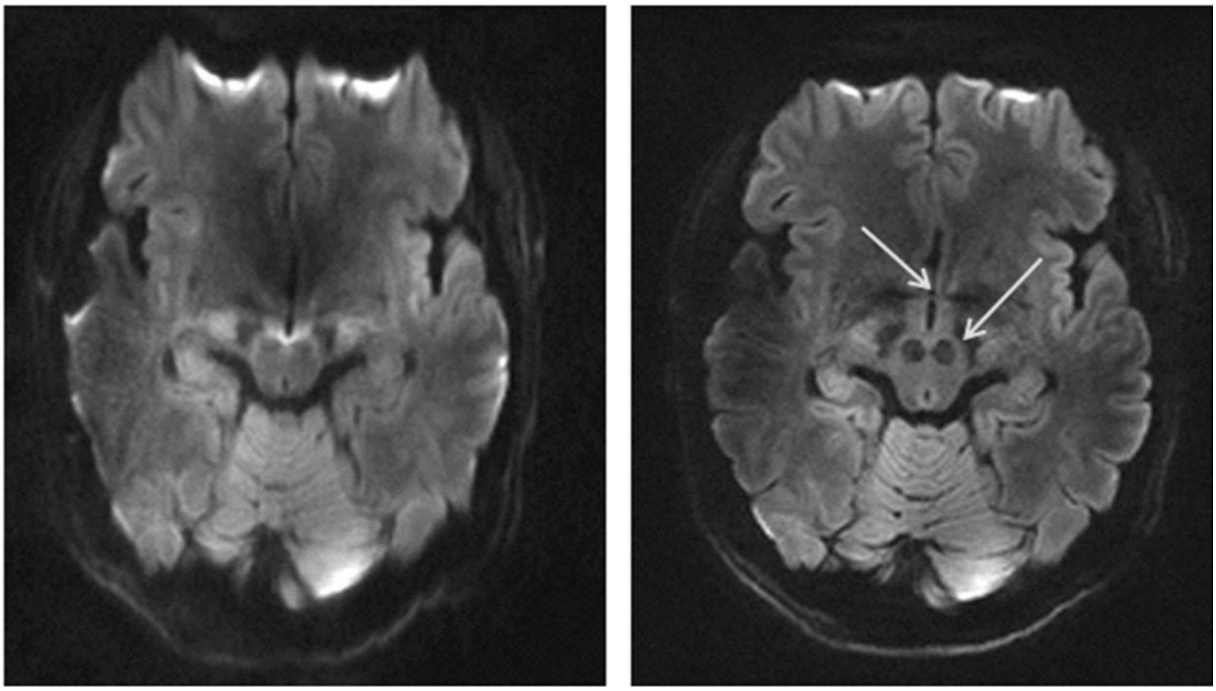

Figure 1. Direct comparison between single-shot EPI (left) and readout-segmented EPI (right) at the base of the brain for a nominal pixel size of 1.1 mm x 1.1 mm x 3.0 mm and a b-value of 1000 s/mm². Both acquisitions are accelerated using GRAPPA with an acceleration factor of three. In the readout-segmented acquisition, anatomical details, such as the anterior commissure (left arrow) and the red nuclei (right arrow) can be clearly identified.

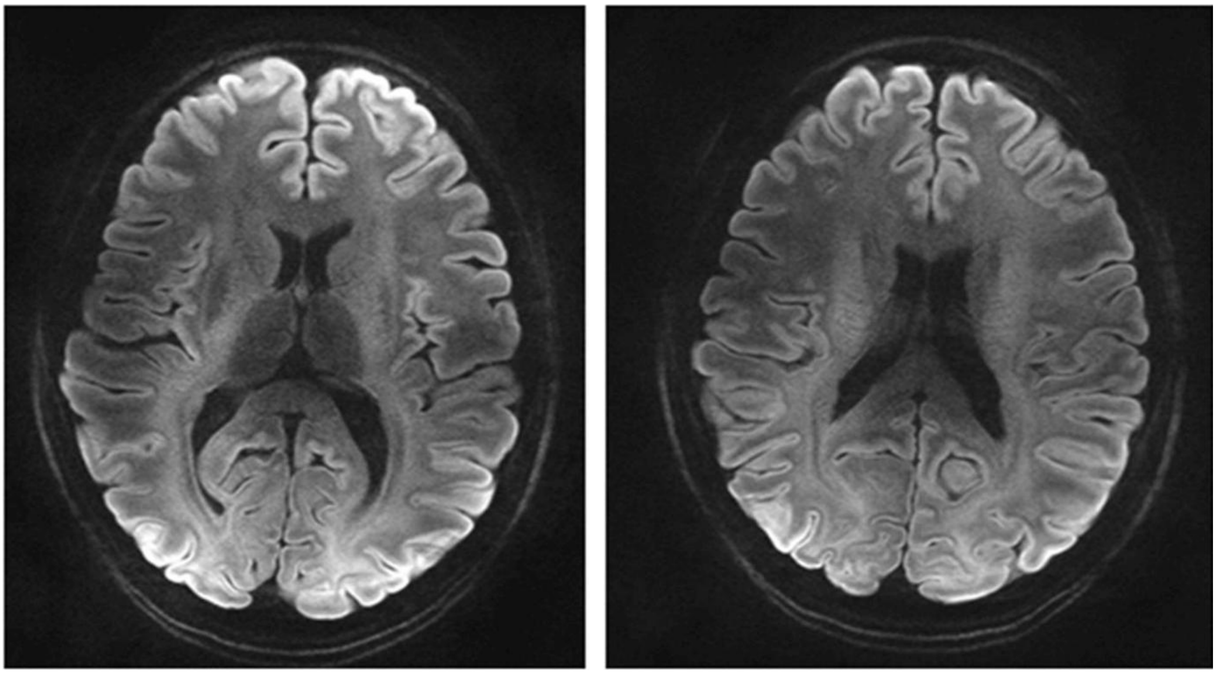

Figure 2. High resolution multi-shot images, acquired using readout-segmented EPI with a nominal pixel size of 0.7 mm x 0.7 mm x 3.0 mm and a b-value of 1000 s/mm^2.

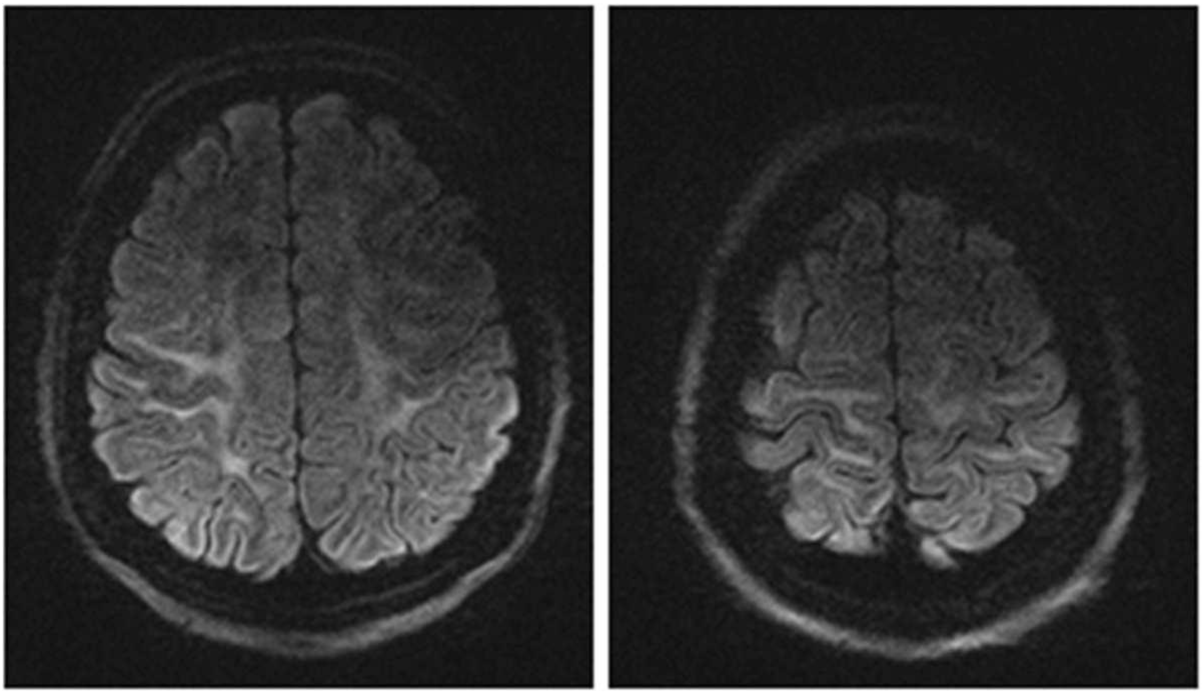

Figure 3. Readout-segmented EPI images for one diffusion gradient direction and one average; taken from the DTI data set obtained with protocol A.

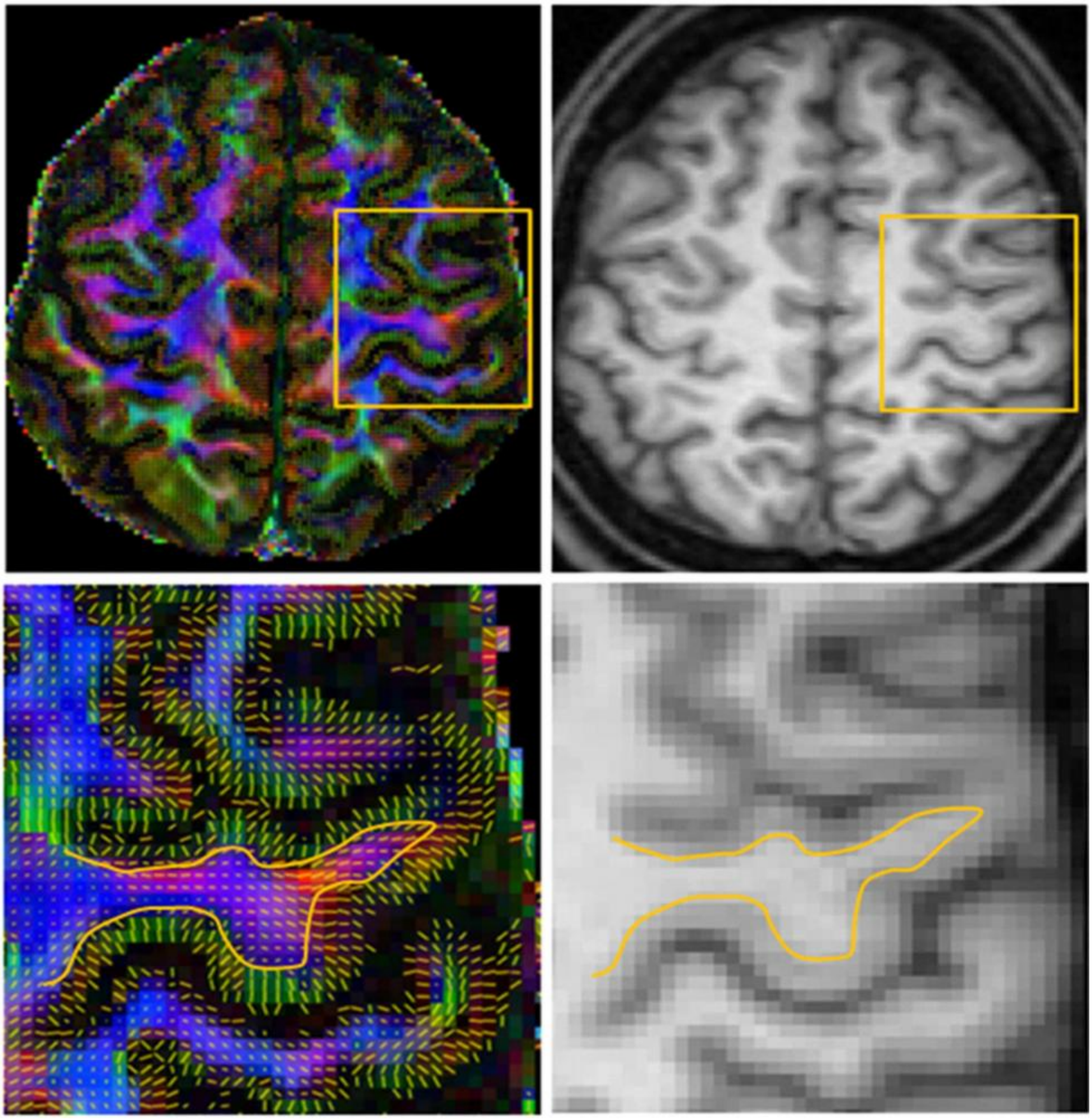

Figure 4. (left) Color coded FA with overlaid vector orientation and (right) corresponding anatomy. (bottom) Enlarged sections showing the precentral gyrus with the gray-white matter interface outlined in yellow.

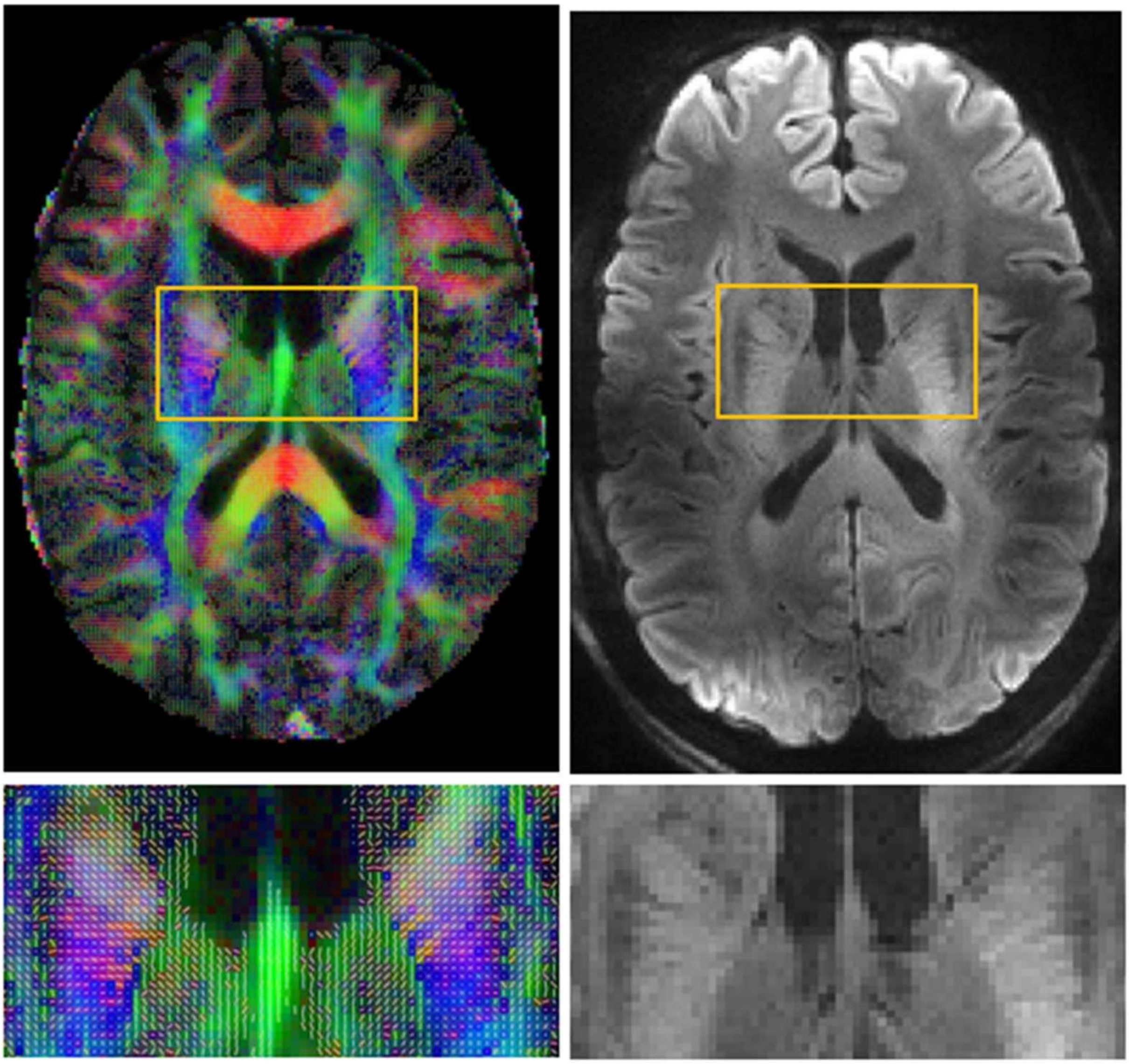

Figure. 5. (left) Color coded FA with overlaid vector orientation and (right) corresponding traceweighted image with a b-value of 1000 s/mm². (bottom) The enlarged sections show the internal capsule.